J Mater Sci: Mater Med (2009) 20:1273–1280
DOI 10.1007/s10856-009-3695-3

A comparative study of the physical and mechanical properties of three natural corals based on the criteria for bone–tissue engineering scaffolds

Yu-Chun Wu · Tzer-Min Lee · Kuo-Hsun Chiu · Shyh-Yu Shaw · Chyun-Yu Yang

Received: 7 September 2007 / Accepted: 20 January 2009 / Published online: 9 March 2009

Abstract Coral has been used for bone grafts since 1970. Because coral has the advantages of good osteoconduction, biocompatibility, and biodegradation, it is also suitable for scaffolds used in bone–tissue engineering. However, the skeletons of different species of corals often vary significantly, and very few studies focus on the assessment of the permeability and mechanical properties of coral structure. In order to better understand the use of coral in bone tissue–engineering, we selected three typical models (*Acropora* sp., *Goniopora* sp., and *Porites* sp.) to analyze for pore size, porosity, permeability, and mechanical strength. We found *Goniopora* and *Porites* had homogenous structure and *Acropora* had oriented pores and irregular pore size. *Acropora* had the largest permeability, however, the transverse section was closed and the useful size was limited because of its habitat type. *Porites* had the smallest pore size and had the lowest permeability. Our data indicated that *Goniopora* sp. can be considered as the most promising source of scaffolds for bone–tissue engineering because of its high porosity (73%) and that its permeability and mechanics were similar to those in human cancellous bone. In conclusion, we analyzed the impact of the macroporous structure of coral on the permeability and mechanical properties that provide indicators for designing the optimal scaffold for bone–tissue engineering.

Y.-C. Wu · S.-Y. Shaw
Institute of Biotechnology, National Cheng Kung University, Tainan 70428, Taiwan

T.-M. Lee
Institute of Oral Medicine, National Cheng Kung University Medical College, Tainan 70428, Taiwan

K.-H. Chiu
Institue of Marine Biology, National Sun Yat-Sen University, Kaohsiung 80424, Taiwan

S.-Y. Shaw (✉)
Department of Chemistry, National Cheng Kung University, Tainan 70428, Taiwan
e-mail: syshaw@mail.ncku.edu.tw

C.-Y. Yang (✉)
Department of Orthopedics, National Cheng Kung University Medical College, Tainan 70428, Taiwan
e-mail: cyyang@mail.ncku.edu.tw

1 Introduction

Autogenous bone has remained the gold standard for restoring bone defects despite its known autograft limitations. For example, second surgery renders the donor site morbid, and the availability of autologous bone is limited [1]. Therefore, bone substitutes provide an alternate solution. A basic bone substitute should be tolerated by the host tissue without any adverse reaction. Coral skeleton is a good biomaterial for bone grafting.

The skeletons of certain reef-building corals, the scleractinians, were used as bone graft substitutes decades ago [2–4]. Their porous structure make them osteoconductive, which allows the ingrowth of fibrovascular and bone tissue [5], and they are biodegradable, which allows their replacement by host bone after resorption [3]. In addition, corals deliver transforming growth factor beta (TGF-β), bone morphogenetic protein, and bone marrow stromal cells, all of which increase osteogenesis, vascularization, and bone regeneration [6–8]. Corals can also be used as good scaffolds for bone tissue engineering [9, 10].

The strategy of bone tissue engineering is to deliver osteoprogenitor cells with a scaffold to the site for bone

regeneration [11]. It is a promising method for an alternative to autograft. We have to take into consideration, when designing scaffolds for bone–tissue engineering, whether the material is sufficiently mechanically strong, easily metabolizes nontoxic waste products, is osteoconductive, and has interconnectively porous architecture.

For the optimal success of bone–tissue engineering scaffolds, the issue of nutrient transport needs to be addressed as well. Pore size and porosity are the traditional parameters used to characterize a scaffold. Pore size and porosity provide space for the cells to grow into the scaffold and for extracellular matrix (ECM) formation. However, the porosity and pore size are not comprehensive intrinsic parameters for describing nutrient transport. Permeability, as described by Darcy's law, is a measure of the ability of a material to transmit fluid. It can be taken as the inflow of nutrients and the elution of metabolic waste. Although a highly porous scaffold is usually highly permeable, scaffolds with similar porosity can have vastly different permeabilities [12]. Permeability is the result of the combination of (1) porosity, (2) pore size and distribution, (3) interconnectivity, (4) fenestration size and distribution, and (5) orientation of pores with respect to flow direction. Permeability is a more comprehensive parameter than pore size and porosity when describing a bone–tissue engineering scaffold.

There are more than 200 species of Taiwan reef-building corals, scleractinian ("hard-rayed") corals, in southern Taiwan [13]. However, little is known about differences between scleractinian species in demand for bone–tissue engineering and the use of Taiwan scleractinians for surgical implantation. The aims of the present study were, first, to evaluate the three typical models of Taiwan scleractinian species (*Acropora grandis*, *Goniopora tenuidens,* and *Porites murrayensis*), based on the criteria for bone–tissue engineering scaffolds, by comparing their differences in pore-size, porosity, permeability, and mechanical strength, and, second, to determine which of these three corals might be of interest for the ideal bone–tissue engineering scaffold.

2 Materials and methods

2.1 Experimental scaffold

The following scleractinian genera have been used as bone graft substitutes: *Pocillopora*, *Acropora*, *Goniopora*, *Montipora*, *Porites*, *Fungia*, *Polyphyllia*, *Favites*, *Acanthastrea*, *Lobophyllia*, and *Turbinaria* [14]. The scleractinian corals we collected in southern Taiwan belonged to the genera *Poccilopora, Acropora, Porites*, and *Goniopora*. To remove the organic tissues of the collected corals, we put them in continuous baths of 3% sodium hypochlorite (NaOCl) solution, washed them with distilled water, and dried them.

2.2 Geometric characterizations

We cut the prepared coral samples using a diamond saw and then ground them to 5 × 5 × 2 mm with a series of SiC sandpapers (3 M). All experiments were done in the isotropic plane of the coral specimens. The isotropic plane is perpendicular to the direction of polyp growth. The geometric characterizations of these sliced samples were done using a stereo optical microscope coupled with a digital camera (Coolpix 4500; Nikon) and a scanning electron microscope (SEM) (XL-40FEG; Philips). We also did microtomography (micro-CT) (model 1076; Skyscan) experiments to reconstruct the 3-dimensional structure of the coral specimens. Acquired images were recorded with the pixel size set to 8.6 μm. Three-dimensional images of corals were reconstructed from a series of 2D images using 2D/3D processing, analysis, and visualization programs (CTAn (v.1.7) + CTVol (v.1.11), 32-bit version for Windows XP; Skyscan).

The bulk density of coral specimen was defined as the ratio of total volume of scaffold divided by weight. The true density was measured using buoyancy method. We ground coral into powder form and measured the volume of powder by immersing in water according to Archimedes principle.

The total porosity was calculated using Eq. 1:

$$p_T = 1 - \frac{\rho_b}{\rho_t} \tag{1}$$

where P_T is the total porosity, ρ_b is the bulk density, and ρ_t is the true density.

The distribution of pore size was measured using image-analysis software (Image-Pro Plus; Media Cybernetics). Pores were measured in a perpendicular direction through the long and transverse axes from SEM microphotographs. We calculated 200 pores for each sample and took the average values as the mean pore size.

2.3 X-ray diffractometry and thermal analysis

The powder samples of *Acropora*, *Goniopora*, and *Porites* were examined with a high resolution X-ray powder diffractometer (XD-D1; Shimadzu). To determine to which temperature it is possible to heat a coral sample for sterilization without altering its crystalline structure, we measured, using differential scanning calorimetry coupled with thermogravimetry measurements from a thermomechanical analyzer (TA-60Ws; Shimadzu).

2.4 Permeability studies

We measured the permeability of coral samples using a previously described method [12, 15]. A fluid under a known pressure is allowed to flow through the porous coral and its flow rate is measured. We measured the flow rate ten times for each kind of coral. We cut the samples using a diamond saw and then, using a series of SiC sandpapers (3 M), ground them into $10 \times 10 \times 5$ mm bars. All specimens were mounted in cylindrical polystyrene tubes $\pi(5\text{ mm})^2$ long $\times$ 5 mm wide. The space between the specimen and the tube was filled with thermal plastic resins. Water pressure was generated by the water level between the reservoir and coral sample top surface and it was 143.4 cm, corresponding to a pressure of 14.07 kPa. The volumetric flow rate (ml/s) through the coral was measured by determining the amount of time 80 ml of water took to flow through the specimen. The permeability was calculated using Darcy's Law as expressed in Eq. 2:

$$K = \frac{QL\mu}{\Delta PA} \tag{2}$$

where κ is the permeability, ΔP is the pressure gradient (kPa) across the specimen, Q is the volumetric flow rate (ml/s), L is the length (cm) of the specimen, A is the cross-sectional area (cm^2), μ is the kinematic fluid viscosity (η/ρ), and the viscosity (η) of water is 0.001 Pa·S.

2.5 Mechanical studies

A compression test using a tensile/compression testing device (AG-I; Shimadzu) revealed a compression rate of 2 mm/min. Testing was done vertically towards the smallest area of the specimen, each of which was approximately 8 mm long, 6 mm high, and 6 mm wide. Compressive strength was calculated from the load-strain curve using the ratio of the ultimate compressive load to the cross-sectional area of the specimen.

2.6 Cell culture and the biocompatibility of coral

The conditionally immortalized human fetal osteoblastic cell line hFOB was obtained from the American Type Culture Collection (ATCC). The cell line was developed by conditionally immortalizing human fetal osteoblasts using a temperature-sensitive mutant of the SV40 large T antigen (*ts-SV40LTA*) gene [16]. The cells were cultured in a 1:1 mixture of phenol-free Dulbecco's modified Eagle's medium/Ham's F-12 medium (Sigma-Aldrich) supplemented with 10% fetal bovine serum (FBS) (HyClone) and G418 sulfate antibiotic (geneticin) (0.3 mg/ml; Promega) at 34°C.

The corals were cut into $4 \times 4 \times 4$ mm cubes and sterilized in an autoclave at 121°C for 20 min. We seeded hFOB onto the sterilized coral at 1×10^5 cells/sample for 1 day. The cell/coral composites were then rinsed several times with cacodylate buffer (pH 7.2), fixed for 2 h with 2.5% glutaraldehyde in 0.1 M of buffered cacodylate (pH 7.2), post-fixed for 1 h in 1% OsO_4 in buffer, dehydrated in an ascending alcohol series, and then immersed in hexamethyldisilazane (HMDS) for 10 min in lieu of critical point drying [17]. Finally, after the cell/coral composites had been sputter-coated with gold, we examined them using a SEM (Hitachi, S-2500).

2.7 Statistical analysis

The results are presented as means ± standard deviation (SD). We used analysis of variance (ANOVA) and then the Student-Newman-Keuls method for all assessments. Statistical significance was set at $P < 0.05$ for all tests.

3 Results and discussion

3.1 Macro- and microstructure and biocompatibility

We collected four genera of coral: *Poccilopora, Porites, Acropora, and Goniopora. Poccilopora* has close pore interconnections, which makes it unsuitable for scaffolds; therefore, we used only *Acropora*, *Goniopora*, and *Porites* in this study. The *Acropora* species belongs to *Acroporidae*, and *Goniopora* and *Porites* species belong to the *Poritidae* family (Table 1). Figure 1 shows the natural habitats of three kinds of coral. *Acropora* sp. (Fig. 1a) have branched and arborescent forms; they comprise the largest number of coral species in all tropical oceans. The skeletons they build, denser than those of *Goniopora* and *Porites,* are not easy to shape, and the size of the scaffold that can be made

Table 1 Classification of corals in biomedical use

Kingdom
Animalia
Phylum
Coelenterata
Order
Scleractinia
Family
Acroporidae (the dominant group of reef-builders)
Indo-Pacific genera
Acropora sp.
Poritidae (the porous nature of the corallum)
Indo-Pacific genera
Goniopora sp.
Porites sp.

Fig. 1 Underwater photographs showing the three marine corals in their natural habitats: **a** *Acropora* sp., **b** *Goniopora* sp., and **c** *Porites* sp

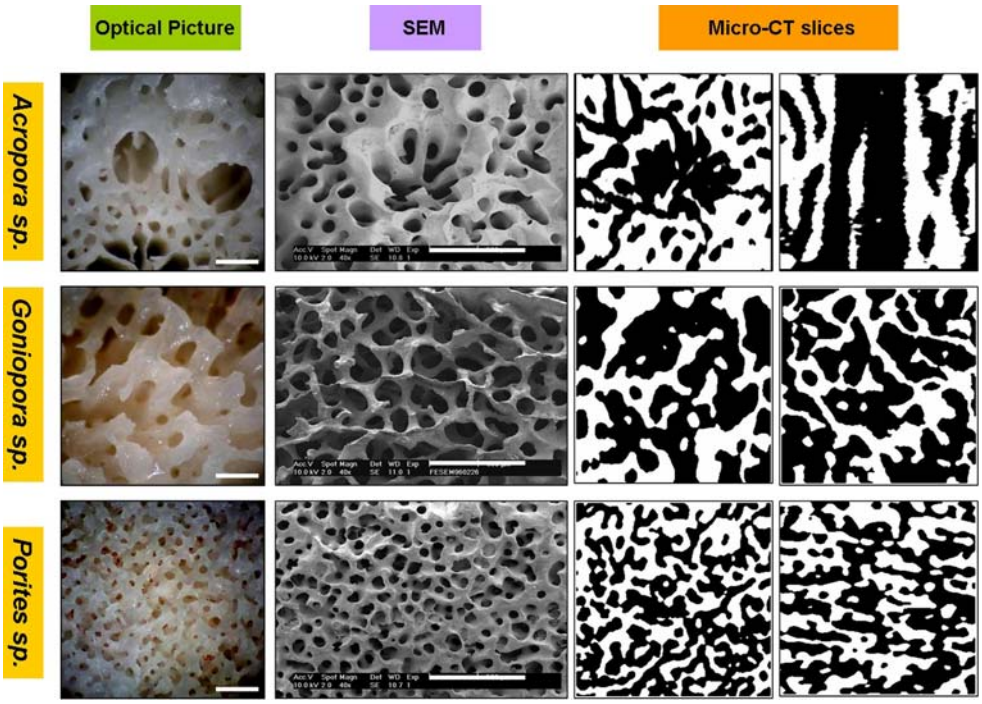

Fig. 2 Two-dimensional image analysis of the three specimens. The scale bar is 1 mm long. Micro-CT slices: the left picture is on the isotropic (x–y) plane; the right picture is on the x–z plane. Image size = 6.7 mm^3

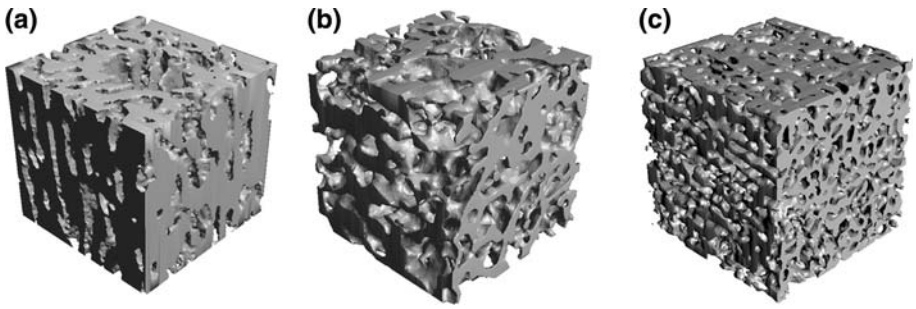

Fig. 3 Three-dimensional graphs of the three specimens (constructed using micro-CT). **a** *Acropora* sp., **b** *Goniopora* sp., and **c** *Porites* sp. The length of the cube is 2580 μm

from an *Acropora* sp. skeleton is limited. *Goniopora* sp. and *Porites* sp. both have a rounded, protuberant, massive form. They grow fast near the seacoast, and can reach 2 m long. They are easily shaped into the desired scaffolds. We cut them into 5 mm cubes and evaluated the structure with optical, SEM, and Micro-CT slices (Fig. 2). *Acropora* had many irregularly shaped pores and the fenestration size was smaller and more closed as compared to *Goniopora* and *Porites*. However, *Acropora* had the largest pore size, and all the pores were similarly oriented, which is helpful in permeability tests (shown as Micro-CT slices in Fig. 2). The walls of *Acropora* and *Goniopora* were thicker than those of *Porites*, which may explain why they performed better on the mechanical test. There is also showed the 3 D model of corals with reconstructed Micro-CT slice in Fig. 3.

Acropora sp. had the largest mean pore size (412 ± 212 μm; range: 124–941 μm), *Goniopora* had the second largest (314 ± 116 μm; range: 145–651 μm), and *Porites* had the smallest (154 ± 53 μm; range: 89–435 μm) (Fig. 4). A pore size of over 100 μm was previously reported as a minimal requirement for fibrovascular

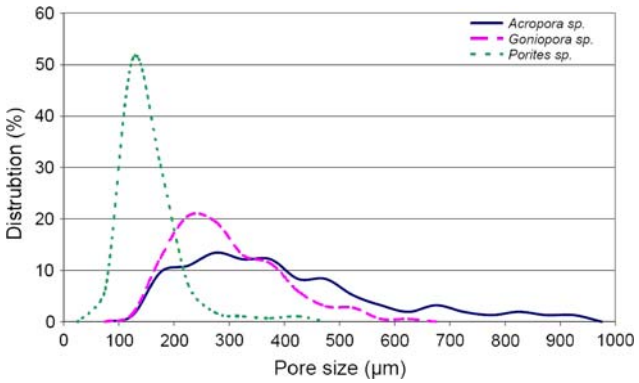

Fig. 4 The pore size distribution of the three specimens

and bone tissue ingrowth [18]. Most of the corals we used met the structural requirements for bone substitute. However, it is under consideration that about 30% of the *Porites* pores are below 100 μm and 100 μm is the minimum for bone ingrowth and angiogenesis. The small pore size (<100 μm) maybe leads the necrotic tissue developing and provide a factor for infection.

We also evaluated the porosity of the coral using density measurements in air and distilled water: *Acropora* was 60.72%, *Goniopora* was 73.80%, and *Porites* was 64.04% (Fig. 5). The porosity of *Goniopora* was highest with a value similar to that of human proximal femur cancellous-bone (73%) [15]. The porosity of a coral skeleton is the main factor for tissue engineering because it partially determines cell-loading capacity [19, 20].

The microstructure of these three corals showed many crystals approximately 2 μm long growing in different directions (Fig. 6). All crystals of these crystals were needle-like form, and *Acropora* crystal was thin, *Porites* crystal was round and *Goniopora* crystal was intermediate. An EDS analysis indicated that the crystals were composed of calcium, carbon, and oxygen, the constituents of calcium

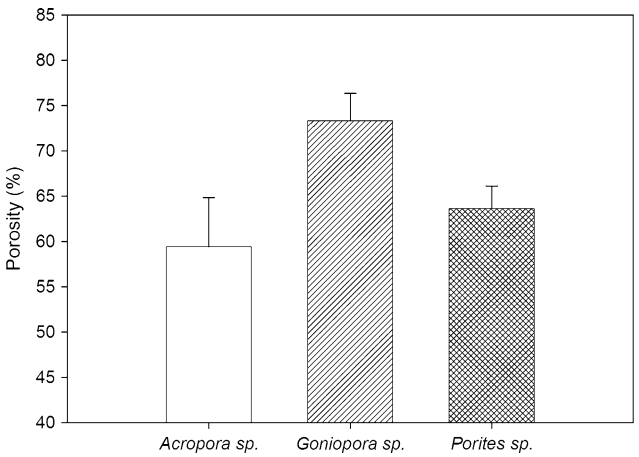

Fig. 5 The porosities of the three specimens ($N = 5$)

carbonate ($CaCO_3$) (data not shown). Osteoclasts produce carbonic anhydrase, which degrades the coral skeleton [3]. We also cultured a human fetal osteoblast cell line (hFOB 1.19) on the corals for 1 day. The osteoblasts cultured on *Acropora* resulted in a rough texture, those on *Goniopora* were more elongated and less flat, and those on *Porites* were polygonal. Whatever the morphology, osteoblasts attached to and grew on all the corals.

3.2 XRD analysis and transition temperature

The XRD patterns of *Acropora*, *Goniopora*, and *Porites* corals are shown in Fig. 7. The stable phase of calcium carbonate at atmospheric pressure is called calcite, which has an R3c structure, while the stable high-pressure phase is called aragonite and has a Pmcn structure. All three of these corals are found only in the aragonite phase. The pre-adipocyte cultured on *Porites lutea* differentiated into an osteogenic phenotype without added bone morphogenesis or inducers [21], which suggests that the 3D bio-matrix morphology, unique crystalline aragonite, and chemical composition of coral may facilitate a favorable bio-mimicking environment for bone-forming cells.

A thermal analysis of the high-temperature behavior of the three corals revealed one significant endothermic peak in Fig. 8. The aragonite structure underwent a phase rearrangement above 290°C; this resulted in the calcite phase. The sterilization temperature of coral is usually 120°C; therefore, sterilization should not change the crystalline phase of corals.

3.3 Permeability and permeability/porosity ratios

Nutrition transmission is a critical factor for tissue engineering scaffolds. Permeability affects the transmission of nutrition, which is normalized by the geometric size of the scaffold and the viscosity of the fluid used. Permeability is affected by a combination of porosity, pore size and distribution, interconnectivity, fenestration size, and the distribution and orientation of the pores with respect to the flow direction [12]. In the present study, *Acropora* had the highest permeability (4.46×10^{-9} m^2) and *Porites* had the smallest (0.12×10^{-9} m^2) (Figs. 9, 10). *Acropora* had the largest pore size, and it may be that pores oriented in the same direction improved fluid conductance. However, there was no water flow when the transverse section of *Acropora* was done. It also may be that pores oriented in the same direction in *Acropora* prevent vertical flow. A specimen with highest permeability is not an optimal scaffold, there are still other considerations, for example low porosity and oriented pores. *Goniopora* and *Porites* did not show the influence of pore orientation. The absolute permeability of 16

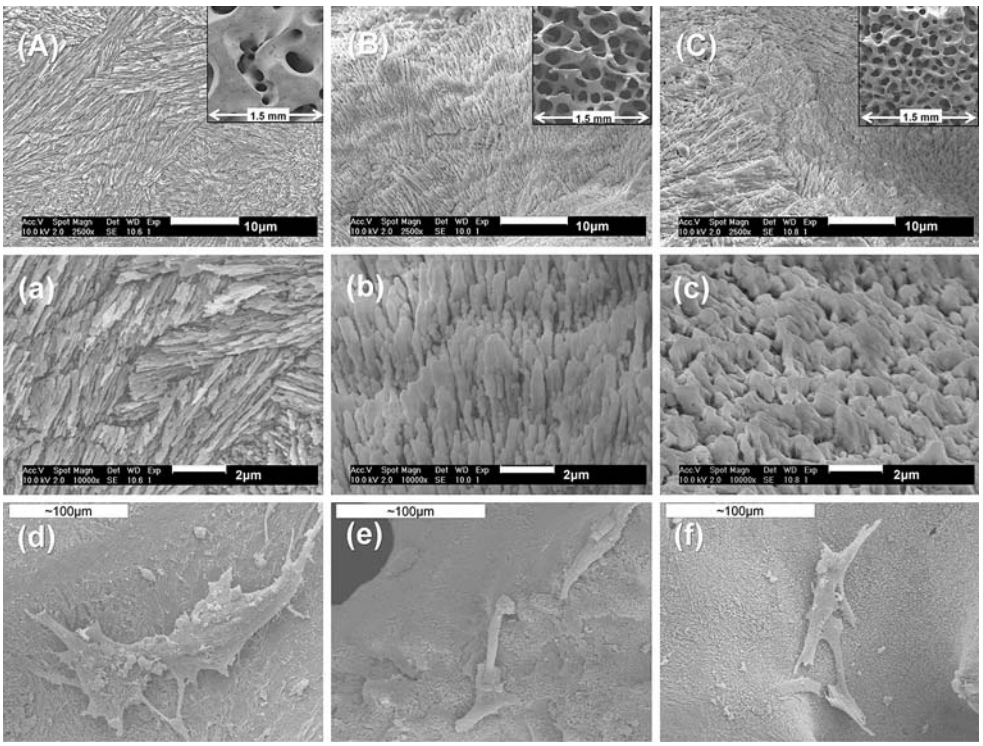

Fig. 6 The microstructures of the three specimens (SEM). **A**, **a** & **d** *Acropora* sp., **B**, **b** & **e** *Goniopora* sp., and **C**, **c** & **f** *Porites* sp. Part **A–C** is the intermediate magnification images of three corals and the inside square shows the low magnification image. Part **a–c** is the high magnification images of three corals. Part **d–f** shows the hFOB cells spread well on the surface of three corals and the morphorgy of osteoblasts on *Acropora* behave a rough texture, those on *Goniopora* were more elongated and less flat, and those on *Porites* were polygonal

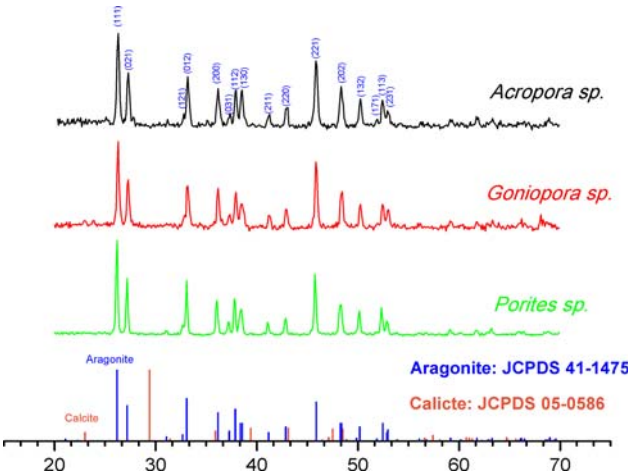

Fig. 7 The X-ray diffraction patterns of the three specimens. The blue color: the standard peaks for aragonite. The orange color: the standard peaks for calcite

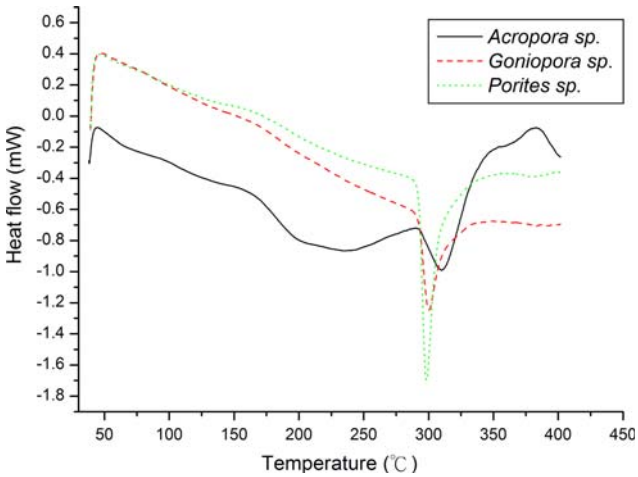

Fig. 8 The DSC curves of the three specimens

human trabecular bones between 32 and 89 years old was reported [15] to be 0.4–11 $\times$ 10^{-9} m^2, which correlated to the specimen porosity (78–92%). The permeability of our *Goniopora* was 0.35 $\times$ 10^{-9} m^2, close to the value (0.4 $\times$ 10^{-9} m^2) of the human proximal femur in the transverse direction, with 78% porosity [15]. The permeability value of *Goniopora* was higher than that of *Porites* because of its large pore-size, fenestration, and higher porosity. High porosity, however, does not imply mechanical strength. In fact, compressive strength decreases as porosity increases [22]. Therefore, taking porosity into consideration, we normalized permeability with porosity to derive a better parameter to characterize

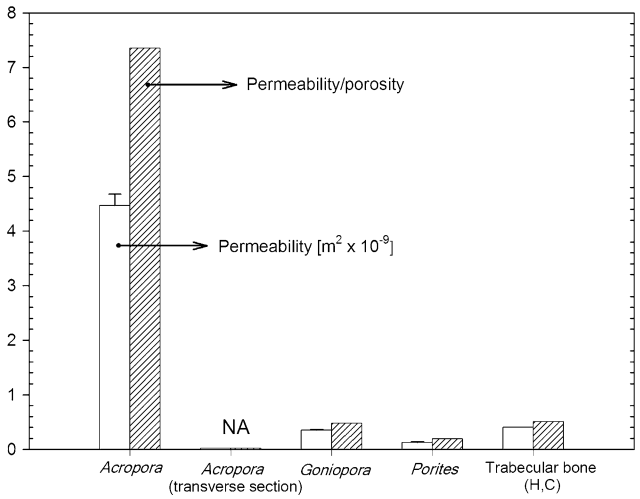

Fig. 9 The permeability and permeability/porosity ratios of the three specimens. All differences are statistically significant ($P < 0.05$) ($N = 10$). For the value of human trabecular bone see [15]; (H,C) = human calcanus

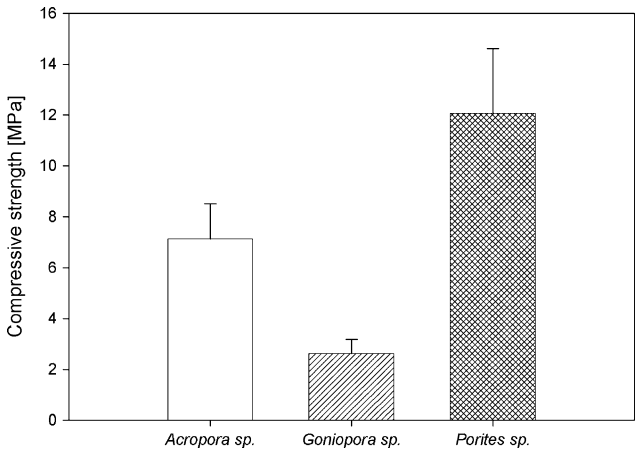

Fig. 10 The compressive strengths of the three specimens. All differences are statistically significant ($P < 0.05$) ($N = 10$)

porous scaffold for tissue engineering. The values for *Acropora*, *Goniopora*, and *Porites* were 7.35, 0.48, and 0.19 [$\times 10^{-9}$ m^2/porosity] respectively.

Alvarez et al. [23] reported the permeability of the *Acropora palmata* coralline species (Elkhorn coral) as 0.369×10^{-11} m^2 and ascribed it to the coral's low porosity (21–28%). This was significantly smaller than our finding (4.46×10^{-9} m^2, Staghorn coral). A micro-computed tomographic (CT) comparative computational analysis of the pore size, permeability, and mechanical properties of *Goniopora* and *Porites* (from Bangkok, Thailand), revealed that *Porites* had a homogeneous structure and some radical anisotropy (pore size: 275, porosity: 53.7%), and that *Goniopora* had a heterogeneous morphology (pore size: 279, porosity: 23.4%) [24]. The porosity value of *Goniopora* in our study (73.8%) and in Demers et al. [25] (80%) were much larger than the 23.4% reported by Knackstedt et al. [24]. The difference is probably due to the structural characteristics of the same genus of coral varies depending upon the habitat types of its provenance and the degree of its petrifaction. After coral dies and petrifies in its natural habitat, its pore size and porosity might decrease, thereby affecting the experimental evaluation of the coral samples. Petrifaction should be taken into consideration when harvesting coral samples. However, Knackstedt et al. [24], Li et al. [12], and the present study all found that permeability positively correlated with porosity.

3.4 Compressive strength of three corals

A key requirement in bone is compressive strength. We found that *Porites* had the highest compressive strength (approximately 12.06 MPa), which may be due to its small pore-size and low porosity. *Goniopora* had the lowest compressive strength (approximately 2.62 MPa), which may be due to its large pore-size and high porosity. The compressive strength of cortical bone varies, and the range of femur bone is between 131 and 283 MPa [26, 27]. Cancellous bone is much weaker than cortical bone, and the results obtained have varied, depending on the location of the bone [28]: the compressive strength of cancellous bone ranged from 1 to 12 MPa. Our findings showed that the compressive strength of all three of the tested corals were within or higher than the range reported for cancellous bone. This finding also showed that different coral species may be used for defects in different types of bones. *Porites* should be used for rectifying defects in bones that demand high compressive strength, but *Goniopora* can be used for defects in bones that demand only low compressive strength.

3.5 Ecological concern

In addition to the medical impact of these corals, we also must pay attention to the role of coral in the ecological system. Coral can form reef to provide the habitat for many marine organisms. However, the pollution and ocean acidification of the world has inevitably resulted in the severe destruction of coral species and ecosystems. In the recent study [29], scientist used massive *Porites* for sclerochronological investigation and find coral calcification in Australian reef has declined by 14.2% since 1990. Scientists have predicted that more than half of the coral reefs in the world may be destroyed by the year 2030 [30]. Therefore, the balance between the economic use and ecosystems of coral reef will be an important issue. Meanwhile, the deterioration of environment will make the coral contain toxic element and cannot be used in

medicine. It will be needed to check the toxic pollution of coral before medical use. To resolve the above problem, the technique to cultivate coral under controlled conditions is worthy of our expectation, however, the cost should be down compared with wild coral.

4 Conclusions

1. We showed that *Acropora* sp., *Goniopora* sp., and *Porites* sp. have different pore sizes and architectures, and that these lead to different permeabilities and compressive strengths. We found that *Acropora* have a largest pore size (412 ± 212 μm), *Goniopora* have a middle mean pore size (314 ± 116 μm), and *Porites* have a smallest pore size (154 ± 53 μm). The *Acropora* show oriented and irregular pores and fenestration size was smaller and more closed. *Goniopora* and *Porites* have even pore distribution and that their structures are the most similar to natural bone.
2. The skeleton of the *Acropora*, *Goniopora*, and *Porites* were all composed by aragonite crystals. The microstructures of these three corals showed 2 μm oriented crystals. The hFOB could culture on these corals and showed the corals have non-cytotoxic elements.
3. In the present study, we found that *Goniopora* sp. had the largest porosity (73%) and that its permeability and mechanics were similar to those in human cancellous bone. Although *Acropora* had the largest permeability, the transverse section was closed and the useful size was limited because of its habitat type. *Porites* had the highest compression strength because of its small pore size; however the small pore size caused lowest permeability. Therefore, *Goniopora* sp. had the largest porosity and suitable permeability and mechanic strength and it can be considered the most promising source of scaffolds for bone–tissue engineering.

Acknowledgements This work was supported in part by grant NSC 93-2320-B-006-071 from the National Science Council, Taiwan. We thank Mr. Bill Franky for help in manuscript preparation and Mr. Chung-Kai Liang for providing the natural photos of Acropora and Porites. We also thank Dr. Keryea Soong for reviewing the manuscript and providing helpful comments.

References

1. E.M. Younger, M.W. Chapman, J. Orthop. Trauma **3**, 192 (1989). doi:10.1097/00005131-198909000-00002
2. A. Patel, F. Honnart, G. Guillemin, J.L. Patat, Chirurgie **106**, 199 (1980)
3. G. Guillemin, J.L. Patat, J. Fournie, M. Chetail, J. Biomed. Mater. Res. **21**, 557 (1987). doi:10.1002/jbm.820210503
4. D. Brasnu, F. Roux, B. Loty, H. Laccourreye, Ann. Otolaryngol. Chir. Cervicofac. **105**, 431 (1988)
5. R.T. Chiroff, E.W. White, K.N. Weber, D.M. Roy, J. Biomed. Mater. Res. **9**, 29 (1975). doi:10.1002/jbm.820090407
6. E. Arnaud, C. De Pollak, A. Meunier, L. Sedel, C. Damien, H. Petite, Biomaterials **20**, 1909 (1999). doi:10.1016/S0142-9612(99)00090-3
7. C.J. Damien, P.S. Christel, J.J. Benedict, J.L. Patat, G. Guillemin, Ann. Chir. Gynaecol. Suppl. **207**, 117 (1993)
8. F.P. Luyten, Y.M. Yu, M. Yanagishita, S. Vukicevic, R.G. Hammonds, A.H. Reddi, J. Biol. Chem. **267**, 3691 (1992)
9. H. Petite, V. Viateau, W. Bensaid, A. Meunier, C. de Pollak, M. Bourguignon, K. Oudina, L. Sedel, G. Guillemin, Nat. Biotechnol. **18**, 959 (2000). doi:10.1038/79449
10. G.E. Holt, J.L. Halpern, T.T. Dovan, D. Hamming, H.S. Schwartz, J. Orthop. Res. **23**, 916 (2005). doi:10.1016/j.orthres.2004.10.005
11. R. Langer, J.P. Vacanti, Science (New York, NY) **260**, 920 (1993)
12. S. Li, J.R. De Wijn, J. Li, P. Layrolle, K. De Groot, Tissue Eng. **9**, 535 (2003). doi:10.1089/107632703322066714
13. C.F. Dai, in *Status of Coral Reefs in the Pacific*, ed. by R.W. Grigg, C. Birkeland (University of Hawaii, Honolulu, 1997), p. 123
14. C. Bouchon, T. Lebrun, J.-L. Rouvillain, M. Roudier, Bull. Inst. Oceanogr. **14**, 111 (1995)
15. M.J. Grimm, J.L. Williams, J. Biomech. **30**, 743 (1997). doi:10.1016/S0021-9290(97)00016-X
16. S.A. Harris, R.J. Enger, B.L. Riggs, T.C. Spelsberg, J. Bone Miner. Res. **10**, 178 (1995)
17. M.A. Malik, D.A. Puleo, R. Bizios, R.H. Doremus, Biomaterials **13**, 123 (1992). doi:10.1016/0142-9612(92)90008-C
18. S.F. Hulbert, F.A. Young, R.S. Mathews, J.J. Klawitter, C.D. Talbert, F.H. Stelling, J. Biomed. Mater. Res. **4**, 433 (1970). doi:10.1002/jbm.820040309
19. T.S. Karande, J.L. Ong, C.M. Agrawal, Ann. Biomed. Eng. **32**, 1728 (2004). doi:10.1007/s10439-004-7825-2
20. V. Karageorgiou, D. Kaplan, Biomaterials **26**, 5474 (2005). doi:10.1016/j.biomaterials.2005.02.002
21. R.Z. Birk, L. Abramovitch-Gottlib, I. Margalit, M. Aviv, E. Forti, S. Geresh, R. Vago, Tissue Eng. **12**, 21 (2006). doi:10.1089/ten.2006.12.21
22. L.J. Gibson, M.F. Ashby, *Cellular Solids: Structure and Properties* (Pergamon Press, Oxford, 1988)
23. K. Alvarez, S. Camero, M.E. Alarcon, A. Rivas, G. Gonzalez, J. Mater. Sci. **13**, 509 (2002). doi:10.1023/A:1014787209506
24. M.A. Knackstedt, C.H. Arns, T.J. Senden, K. Gross, Biomaterials **27**, 2776 (2006). doi:10.1016/j.biomaterials.2005.12.016
25. C. Demers, C.R. Hamdy, K. Corsi, F. Chellat, M. Tabrizian, L. Yahia, Biomed. Mater. Eng. **12**, 15 (2002)
26. D.T. Reilly, A.H. Burstein, J. Bone Joint Surg. Am. **56**, 1001 (1974)
27. D.T. Reilly, A.H. Burstein, J. Biomech. **8**, 393 (1975). doi:10.1016/0021-9290(75)90075-5
28. S.A. Goldstein, J. Biomech. **20**, 1055 (1987). doi:10.1016/0021-9290(87)90023-6
29. G. De'ath, J.M. Lough, K.E. Fabricius, Science **323**, 116 (2009). doi:10.1126/science.1165283
30. B. Norlander, Science World (2003)